

# Photochemical & Photobiological Sciences

Accepted Manuscript



This is an *Accepted Manuscript*, which has been through the Royal Society of Chemistry peer review process and has been accepted for publication.

*Accepted Manuscripts* are published online shortly after acceptance, before technical editing, formatting and proof reading. Using this free service, authors can make their results available to the community, in citable form, before we publish the edited article. We will replace this *Accepted Manuscript* with the edited and formatted *Advance Article* as soon as it is available.

You can find more information about *Accepted Manuscripts* in the [Information for Authors](#).

Please note that technical editing may introduce minor changes to the text and/or graphics, which may alter content. The journal's standard [Terms & Conditions](#) and the [Ethical guidelines](#) still apply. In no event shall the Royal Society of Chemistry be held responsible for any errors or omissions in this *Accepted Manuscript* or any consequences arising from the use of any information it contains.

## Photophysics and Photochemistry of cis- trans-Hydroquinone, Catechol and Their Ammonia Clusters: a Theoretical Study

Mitra Ataelahi, Reza Omidyan\* and Gholamhasan Azimi

Department of Chemistry, University of Isfahan, 81746-73441 Isfahan, Iran.

### Abstract

Excited state hydrogen transfer in the Hydroquinone- and Catechol-ammonia clusters has been extensively investigated by the high level *ab initio* methods. The potential energy profiles of the titled systems, at the different electronic states have been determined at the MP2/CC2 levels of theory. It has been predicted that the double hydrogen transfer (DHT) takes place as the main consequence of photoexcited tetra-ammoniated systems. Consequently, the DHT processes, lead the excited systems to the  $^1\pi\sigma^*$ - $S_0$  conical intersections, which is responsible for the ultrafast non-radiative relaxation of UV-excited clusters to their ground states. Moreover, according to our calculated results, the single hydrogen detachment or hydrogen transfer process essentially governs the relaxation dynamics of smaller sized clustered systems (mono- and di-ammoniated).

**Keywords:** trans-Hydroquinone, cis-Hydroquinone, Catechol, Ammonia clusters, Excited states, Hydrogen transfer, Conical intersection.

### 1-Introduction

Excited state hydrogen detachment (ESHD) is an essential mechanism in the photochemistry of aromatic molecules, containing a heteroatom such as oxygen, nitrogen and sulfur and excited state hydrogen transfer (ESHT) is the equivalent mechanism in clusters formed with H acceptor solvent molecules such as water and ammonia<sup>1</sup>. Ammonia is a better hydrogen acceptor than

---

\*Corresponding author, E-mail: [r.omidyan@sci.ui.ac.ir](mailto:r.omidyan@sci.ui.ac.ir), [reza.omidyan@u-psud.fr](mailto:reza.omidyan@u-psud.fr), Fax: (+98) 311 6689732

water. Thus, phenol-ammonia clusters have been attracting many interesting studies due to their intracuster proton transfer reaction<sup>2-4</sup>. Moreover, the study of relatively small solvent-ammonia clusters can thus reveal phenomena that occur in water for larger cluster sizes. However, ESHD, and ESHT processes, owing to their important role in chemistry and biochemistry<sup>5</sup>, have been extensively studied due to their practical uses in many applications, such as fluorescent probes<sup>6</sup>, photostabilizers<sup>7</sup>, dyes<sup>8</sup> and also light-emitting devices<sup>9</sup>.

Phenol is the chromophore of amino acid tyrosine and its photophysical behavior has thus been the subject of numerous studies<sup>1, 10-13</sup>. Phenol exhibits low fluorescence quantum yields<sup>14</sup>, but strong ultraviolet (UV) absorption associated with  $^1\pi\pi^*$  excitations indicating the operation of one or more non-radiative deactivation mechanisms from the photoexcited state(s). The most prominent mechanism involves deactivation via a  $^1\pi\sigma^*$  potential energy surface (PES), which is dissociative along the O-H stretching coordinate, RO-H<sup>1, 11</sup>. The H atom time-of-flight (TOF) spectra, recorded by Ashfold and coworkers<sup>15, 16</sup> confirmed the predicted O-H bond cleavage mediated by the  $^1\pi\sigma^*$  state in phenol and its derivatives. Similar results were observed by Tseng *et al.*<sup>13</sup> in the photo-dissociation of *p*-CH<sub>3</sub>-PhOH using multimass ion imaging technique. More investigations of ESHD, in *para* halogenated phenols by H (Rydberg) atom photofragment translational spectroscopy yielded similar results to those obtained on bare PhOH by Ashfold *et al.*<sup>17</sup>. In addition, the relaxation dynamics of phenolic systems with ammonia clusters has been extensively studied by several groups so far<sup>18-23</sup>. Although the earlier experimental results have been interpreted based on the excited state proton transfer (PT) process from phenol to ammonia<sup>24, 25</sup>, it has been demonstrated that a neutral hydrogen transfer takes place after electronic excitation of phenol-ammonia clusters<sup>26-28</sup>. Therefore, it is now well established that a neutral hydrogen release is the main consequence of photoexcited phenol, pyrrole, indole and so forth<sup>26, 28-31</sup>. In all of these cases, the  $^1\pi\sigma^*$  state governs the hydrogen transfer to the solvent or hydrogen detachment process<sup>32</sup>.

Hydroquinone (1, 4-dihydroxybenzene, HQ) and Catechol (1, 2-dihydroxybenzene, CTC) are prototypical polyhydroxybenzene: molecules containing two (or more) OH moieties pendant to a benzene ring. They are everywhere present in biological systems, constituting the chromophores of several hormones and neurotransmitters such as adrenaline and dopamine. Also, they are the active components of many antioxidants<sup>33</sup>. Due to extraordinary interest in the biochemical

activity of poly-hydroxybenzene<sup>34</sup>, it is important also to investigate their photochemical behavior.

In spite of their importance, rare reports have been devoted on photophysics and photochemistry of titled molecules. The UV absorption spectra of these molecules, were first reported by Beck in 1950<sup>35</sup>. Also, one of the earliest efforts on recording the electronic spectra of these systems in molecular beam, has been made by Lubman and coworkers<sup>36</sup> who recorded (1+1) REMPI spectra of CTC/HQ systems. In addition, few spectroscopic reports have been devoted on the  $S_1$  state of Catechol<sup>37, 38</sup>, and Hydroquinone<sup>39, 40</sup> systems. In Catechol, a hydrogen bonding interaction between one of the OH groups and the adjacent O atom is the reason why a planar  $S_0$  conformer is present in the gas-phase at room-temperature<sup>41, 42</sup>. Also, Hydroquinone has two planar  $S_0$  conformers (namely cis- trans-Hydroquinone) that are present even under jet-cooled molecular beam conditions (see Figure 1). Similar to phenol, the equilibrium geometry of  $S_1$  excited state of Hydroquinone is also found to be planar<sup>43</sup>. Recently, Ashfold and coworkers investigated in detail the  $S_1$  ( $^1\pi\pi^*$ )/ $S_2$ ( $^1\pi\sigma^*$ ) excited state dynamics in Catechol<sup>44</sup>, at a range of excitation wavelengths between 280 nm (the  $S_1$  origin) and 193 nm. It has been demonstrated that O–H bond cleavage proceeds via H atom tunneling from the photo-prepared  $^1\pi\pi^*$  state into the lowest  $^1\pi\sigma^*$  state of the molecule. Additionally, the excited-state lifetimes of different vibronic levels in the first excited state of jet-cooled Catechol have been measured by C. Jouvét *et al.*<sup>45</sup>. It has been reported that the lifetime of the  $S_1$  state is very short, indicating a strong vibronic coupling between the bound  $^1\pi\pi^*$  and dissociative  $^1\pi\sigma^*$  states<sup>45</sup>.

In present study, we report new results on the single and double hydrogen transfer processes in Hydroquinone- and Catechol ammonia clusters. Thus, after summarizing the computational methods, we present the ground- and excited-state optimized structures. We explain the hydrogen detachment and hydrogen transfer processes in HQ/CTC monomers and their clusters with 1-4 ammonia molecules respectively. We emphasize that it has not been the goal of the present study to perform highly accurate calculations of reaction enthalpies and geometric structures of reactants and products. We have rather been interested in the development of a clear qualitative picture of the basic mechanisms of the hydrogen detachment (or transfer) processes in HQ/CTC and their clusters with ammonia.

## 2- Computational details:

The “*ab initio*” calculations have been performed with the TURBOMOLE program suit<sup>46, 47</sup>, making use of the resolution-of-identity (RI) approximation for evaluation of the electron repulsion integrals. The equilibrium geometry of all systems at the ground state has been determined at the MP2 (Moller-Plesset second order perturbation theory)<sup>48</sup> level. Excitation energies and equilibrium geometry of the lowest excited singlet states have been determined at the RI-CC2 (the second-order approximate coupled-cluster method)<sup>49</sup>. The excitation energies and oscillator strengths have been determined by the aug-cc-pVDZ<sup>50</sup> basis function. Furthermore, the potential energy profiles have been calculated at the MP2, CC2/TZVP level of theory, respectively for the ground and excited states.

The abbreviations tHQ, cHQ and CTC have been used, respectively for trans-Hydroquinone, cis-Hydroquinone, and Catechol. Also, the ammonia clusters have been represented by HQ-(NH<sub>3</sub>)<sub>n</sub>/CTC-(NH<sub>3</sub>)<sub>n</sub>; n represents to the number of ammonia molecules.

Ground state geometry optimization of tHQ, cHQ and CTC were performed under symmetry constraint with the *C<sub>s</sub>* molecular symmetry. Within the *C<sub>s</sub>* point group, the wave function of the <sup>1</sup>ππ\* and <sup>1</sup>πσ\* states transform according to the A' and A'' representations, respectively; thus, the excited states can be well-distinguished. The geometry optimization of excited states was carried out with *C<sub>s</sub>* symmetry restriction. In order to optimize the excited state geometries, the optimized structure of the ground state has been selected as the starting point for two lowest excited states of A' and A'' character. To determine barrier heights of the potential energy surfaces, a set of calculations, without symmetry, was performed, that will be addressed as well.

CC2 is the method of choice because it gives reasonable results for medium size organic molecules, either in bare form or in their complex forms (e. g with water and ammonia) for a moderate computational time<sup>51-54</sup>. Comparing the CC2 results with those of the multi-reference CASPT2 approach, the validity of CC2 as a single-reference electronic structure method for determination of PE profiles and qualitative prediction of conical intersections has been confirmed by Sobolewski *et al.*<sup>55-58</sup>.

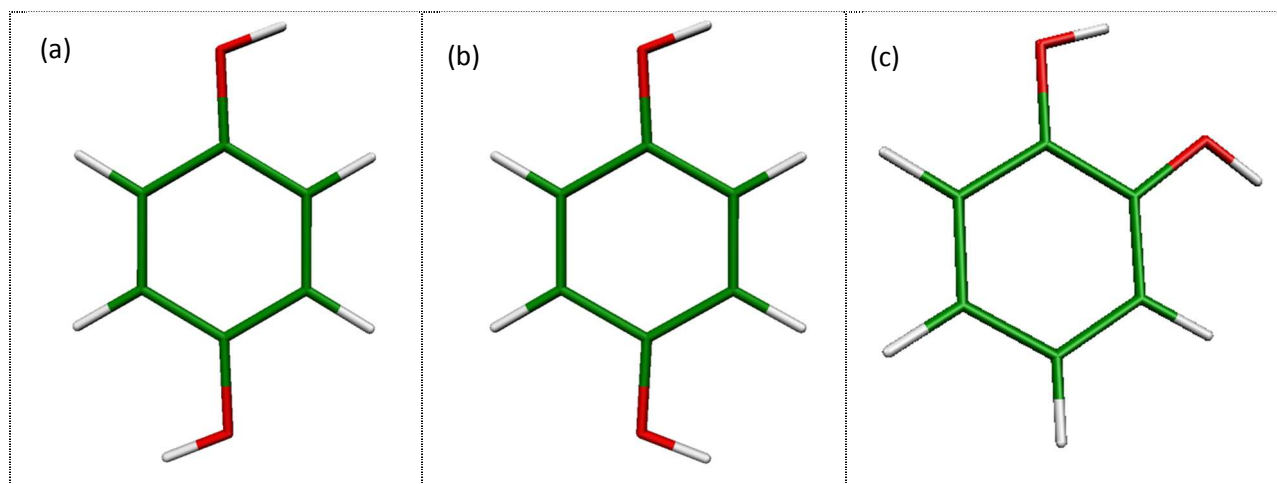


Figure 1. Ground state optimized geometries of: (a) *trans*-Hydroquinone, (b) *cis*-Hydroquinone, and (c) Catechol, calculated at the MP2/aug-cc-pVDZ level of theory.

### 3- Results and discussion:

#### 3-A) Ground and excited-state optimized geometry of individual HQ/CTC and their clusters with ammonia:

The ground state structures of the two isomers of Hydroquinone were determined by microwave spectroscopy<sup>36, 59</sup> and *ab initio* calculations<sup>60-62</sup>. According to the MP2 calculations of Kim *et al.*<sup>63</sup>, it has been reported that *trans*-Hydroquinone is around  $40\text{ cm}^{-1}$  ( $\sim 5\text{ meV}$ ), more stable than its *cis* analogue. This is in good agreement with our calculated results at the MP2/aug-cc-pVDZ level of theory; ( $\Delta E_{(\text{trans/cis})} = -4.5\text{ meV}, 35.8\text{ cm}^{-1}$ ). Also, it has been determined that *cis-trans* conversion has a barrier of  $789\text{ cm}^{-1}$  ( $\sim 0.1\text{ eV}$ ) height.

In addition, the ground state structure of Catechol (CTC) has been investigated by several authors<sup>42, 64, 65</sup>. The planarity of the molecule has been verified in both experimental and theoretical reports<sup>41, 42</sup>. The recorded microwave spectrum together with the vibrational analysis of the O–H stretching band of the molecule, confirm the planar structure of  $C_s$  symmetry as the most stable conformation of the molecule in the gas phase<sup>38, 66</sup> (see Figure 1).

Although, rarely reports have been devoted on HQ/CTC ammonia clusters, the ground-state structure of the tHQ-(NH<sub>3</sub>), has been discussed in detail<sup>67-69</sup>. It has been shown that the complex is planar in electronic ground state, with a nearly linear hydrogen bond between NH<sub>3</sub> and one of

the hydroxyl hydrogen atoms of Hydroquinone. However, on our knowledge, no study has been reported on the larger sized clusters of HQ/CTC with ammonia ( $n \geq 2$ ) in literature.

In order to obtain information on the cluster size dependence hydrogen-transfer processes in HQ- and CTC-(NH<sub>3</sub>)<sub>n</sub> systems, we have investigated their tetra ammoniated complexes (HQ-(NH<sub>3</sub>)<sub>4</sub>, CTC-(NH<sub>3</sub>)<sub>n</sub>). As mentioned above, the *C<sub>s</sub>* symmetry constraint is a necessity for excited-state geometry optimizations. Also, it has been well established that the photophysical aspects of hydrogen transfer in clustered systems is not strongly dependent on the initial geometry<sup>11</sup>.

In Figure 2, we have depicted the optimized ground state structures of clustered systems of HQ and CTC with 2 and 4 ammonia molecules. Because, the individual systems of HQ and CTC are planar, their clustered systems have been constructed from 2 and 4 ammonia molecule(s), connected to HQ/CTC molecules via strong hydrogen bond. Thus, in the M-(NH<sub>3</sub>) and M-(NH<sub>3</sub>)<sub>2-4</sub>, (M, indicates to HQ and CTC), there are one and more OH...HN strong hydrogen bond(s), respectively. Finally, three and tetra-ammoniated clusters of HQ and CTC systems have been constructed by adding more ammonia molecules to the first ones. Since, exact analysis of geometry structures is not the goal of this work, we do not present more discussion on geometry parameters of the ground state clusters; (more information is presented in the ESI file).

We stress once more that the structure shown in Figure 2 are not the lowest energy structure of the tHQ-(NH<sub>3</sub>)<sub>4</sub> and CTC-(NH<sub>3</sub>)<sub>4</sub> clusters. Nevertheless, these structures represent true local minimum of the S<sub>0</sub> surface.

The CC2 geometry optimization at the S<sub>1</sub> (<sup>1</sup>ππ\*) state of the cluster systems does not show remarkable change in geometry parameters, but, via the S<sub>2</sub> (<sup>1</sup>πσ\*) state optimizations, the hydrogen detachment and hydrogen transfer processes have been predicted, respectively for bare and clusters of HQ/CTC systems. The S<sub>2</sub> (<sup>1</sup>πσ\*) state optimization for cHQ-(NH<sub>3</sub>)<sub>4</sub> and CTC-(NH<sub>3</sub>)<sub>4</sub> is accompanied with double hydrogen transfer from the hydroxyl groups to the adjacent ammonia molecules, which produce two radical systems of NH<sub>4</sub>(NH<sub>3</sub>)•, while single hydrogen detachment or hydrogen transfer is the main consequence of the S<sub>2</sub> (<sup>1</sup>πσ\*) optimizations of smaller-sized cluster systems (see ESI file).



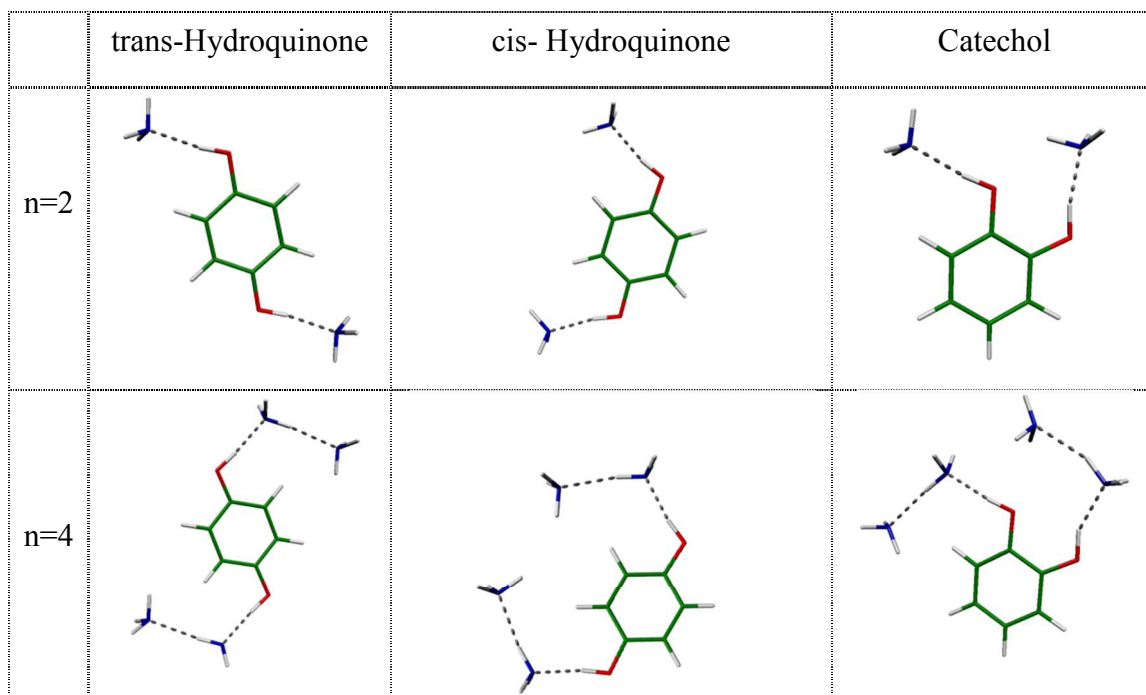


Figure 2: Ground state optimized structures of cis- trans-Hydroquinone-ammonia [HQ-(NH<sub>3</sub>)<sub>n</sub>] and , Catechol-ammonia [CTC-(NH<sub>3</sub>)<sub>n</sub>] clusters, with n=2,4, under the C<sub>s</sub> symmetry constraint.

It should be noted that the charge distribution of the  $\sigma^*$  orbital is located significantly out of the atomic frame (see Figure 3). The  $^1\pi\sigma^*$  excitation is therefore of considerable charge transfer (CT) character. This CT character of the  $^1\pi\sigma^*$  state and the antibonding nodal character of the  $\sigma^*$  orbital provide the driving force for the hydrogen transfer processes.

### 3-B) Vertical and adiabatic transition energies and electronic structures:

Vertical and adiabatic transition energies of the first  $^1A'$  ( $^1\pi\pi^*$ ) and  $^1A''$  ( $^1\pi\sigma^*$ ) excited states have been determined for individual and clusters of HQ/CTC systems at the CC2 level, using aug-cc-pVDZ. The calculated results on individual HQ/CTC molecules have been presented in Table 1. According to the C<sub>s</sub> symmetry point group, which considered for the evaluation of all excitation energies, the excited states belong either to A' or A'' representations. The vertical transition energies were calculated on the optimized geometry of the ground states, while the adiabatic transition energies relevant to the S<sub>1</sub>-( $^1A'$ ,  $^1\pi\pi^*$ ) and S<sub>2</sub>-( $^1A''$ ,  $^1\pi\sigma^*$ ) excited states, were



calculated at the corresponding  $1(^1A')$  and  $1(^1A'')$  excited state optimized geometries respectively.

In order to evaluate the method and basis sets, the electronic transition energies of HQ and CTC, have been calculated and compared with corresponding experimental data<sup>36, 67</sup>. As shown in Table 1, there is well agreement between experimental band origin of  $S_1$ - $S_0$  electronic transition and our calculated values for trans-, cis-HQ and CTC species calculated at the CC2/aug-cc-pVDZ level of theory.

Furthermore, according to the RI-CC2 calculations, in both HQ, CTC systems, the first  $^1A'$  ( $^1\pi\pi^*$ ) state is dominated by the excitation from Homo (the highest occupied molecular orbital) to Lumo (the lowest unoccupied molecular orbital) (~92%). Also, the first  $^1A''$  state has the same nature in HQ and CTC, ( $^1\pi\sigma^*$ ) which is a dark state, and mostly corresponds to the Lumo+2 $\leftarrow$ Homo transition in HQ and Lumo+1 $\leftarrow$ Homo transition in CTC (~ 90%, see ESI file).

	tHQ		cHQ		CTC	
	$S_1(^1\pi\pi^*)$	$S_2(^1\pi\sigma^*)$	$S_1(^1\pi\pi^*)$	$S_2(^1\pi\sigma^*)$	$S_1(^1\pi\pi^*)$	$S_2(^1\pi\sigma^*)$
Vertical transitions (Oscillator strength)	4.42 (0.0540)	4.91 (0.0000)	4.43 (0.0534)	4.84 (0.0000)	4.78 (0.0432)	4.94 (0.0023)
Adiabatic transitions/eV	4.21	----	4.22	----	4.57	---
<sup>#</sup> Exp./ eV cm <sup>-1</sup>	<b>4.153</b> <b>33500</b>		<b>4.158</b> <b>33535</b>		<b>4.419</b> <b>35646</b>	

Table 1: Excitation transition energies (vertical and adiabatic) and oscillator strengths, of HQ and CTC systems, computed at the MP2/CC2 levels, using aug-cc-pVDZ basis function. <sup>#</sup>The experimental values for the 0-0 band of  $S_1$ - $S_0$  transition of HQ/CTC, have been adopted from Ref. <sup>67</sup> and Ref. <sup>36</sup> respectively. The adiabatic values for the  $S_2(^1\pi\sigma^*)$ , has not been reported, since of the large geometry deformation at  $^1\pi\sigma^*$  state.

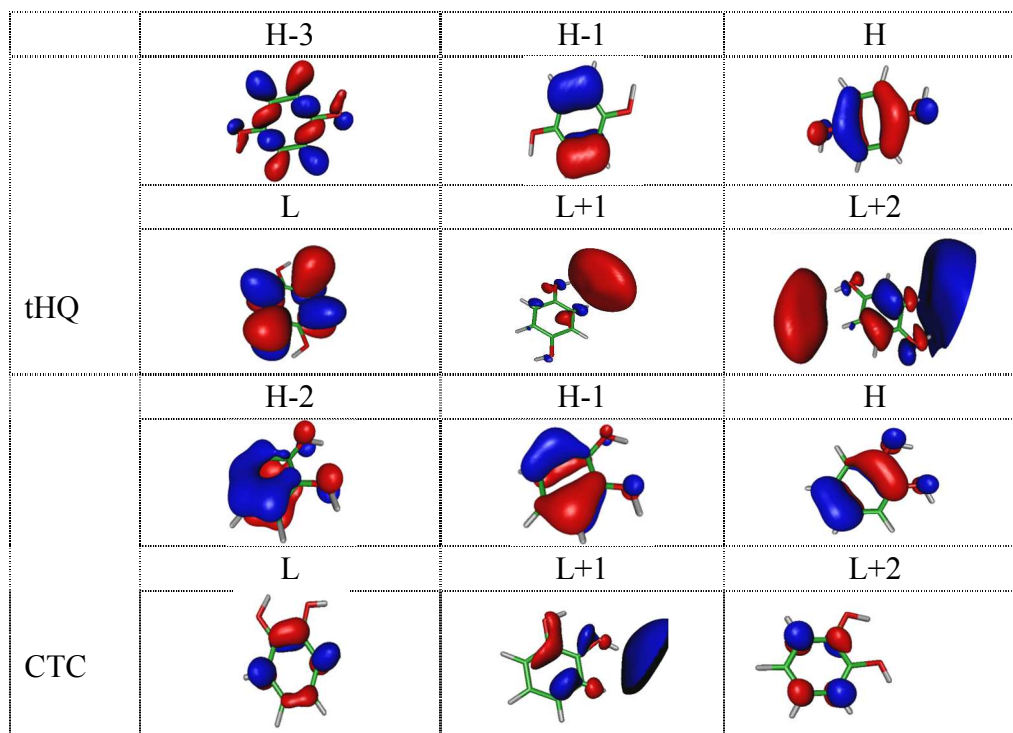


Figure 3: Visualized frontier molecular-orbitals of *trans*-Hydroquinone and Catechol systems, calculated at the SCF/TZVP level of theory. H and L indicate the highest occupied and the lowest unoccupied molecular orbitals, respectively.

In addition, in cluster systems of HQ-(NH<sub>3</sub>)<sub>n</sub> (n=1-3), the S<sub>1</sub> (1A') state corresponds to Lumo←Homo transition, (Lumo and Homo stand for the lowest unoccupied and the highest occupied molecular orbitals, respectively), while in the HQ-(NH<sub>3</sub>)<sub>4</sub> the S<sub>1</sub>-S<sub>0</sub> transition is giving rise to a single electron transition from Homo to Lumo+1 (see ESI file). Also, the S<sub>1</sub> (1A') state in CTC-(NH<sub>3</sub>)<sub>4</sub> originates from a single electron transition of Lumo+2←Homo. However, the S<sub>2</sub> (1A'') state corresponds to electron transition from Homo to L+3, L+1 and L, respectively for HQ-(NH<sub>3</sub>)<sub>1</sub>, HQ-(NH<sub>3</sub>)<sub>2</sub> and HQ-(NH<sub>3</sub>)<sub>4</sub> clusters. For all cluster systems of CTC-(NH<sub>3</sub>)<sub>1-4</sub>, the S<sub>2</sub> (1A'') state mostly corresponds to the single electron transition from Homo to Lumo. The S<sub>1</sub> (1A') and S<sub>2</sub> (1A'') states of monomers and all ammonia clusters of HQ and CTC molecules have been assigned respectively to <sup>1</sup>ππ\* and <sup>1</sup>πσ\* states (ESI file).

Moreover, the electron densities of HOMO and LUMO are entirely localized on the benzene moiety, thus, the  $S_1$  state of the complexes is a locally excited (LE) state, while the electron densities of  $\sigma^*$  orbitals are mostly localized on ammonia molecule(s). So it can be confirmed that the  $S_2$  state of the clusters has a charge transfer (CT) nature; from phenolic part of the complex (HQ/CTC) to its ammonia molecules.

### 3-C) Potential energy profiles:

#### 3-C- I) Hydroquinone and catechol:

In Figure 4 (a, b), the CC2 PE profiles calculated along the minimum-energy path for detachment of hydrogen atom of the OH group of HQ and CTC are shown. For clarity, only the electronic ground state and the lowest  $^1\pi\pi^*$ ,  $^1\pi\sigma^*$  states are presented. The excited state geometries have been optimized along the reaction path, while the ground-state energies have been computed at the  $^1\pi\sigma^*$  optimized geometries. Inspection of the results presented in Figure 4, reveals that the potential energy profiles of ground state and the lowest  $^1\pi\pi^*$  excited state rise with increasing OH distance in an approximately parallel manner, while the PE profile of the  $^1\pi\sigma^*$  state shows repulsive character. The repulsive  $^1\pi\sigma^*$  PE profile crosses with the  $^1\pi\pi^*$  profile at the beginning of the reaction path and subsequently with the PE profile of ground state at the longer distance of OH bond. In a multidimensional picture, the  $^1\pi\pi^*$ - $^1\pi\sigma^*$  and  $^1\pi\sigma^*$ - $S_0$  curve crossings shown in Figure 4 will develop into the conical intersections (CIs).

Because, the potential energy curves of the different electronic states ( $^1\pi\pi^*$ , and  $^1\pi\sigma^*$ ), have been determined independently at different geometry optimizations, the energetic position of  $^1\pi\pi^*$ - $^1\pi\sigma^*$  CIs cannot be exactly determined from Fig. 4.

Nevertheless, the CC2 calculations are reliable<sup>57, 58</sup>, and our results relevant to the CIs provide good evidences to predict the regions of conical intersections, qualitatively. However, only the CIs of  $^1\pi\sigma^*$ - $S_0$  are real, because the relevant PE profiles have been determined at the same geometry optimization.

The calculated adiabatic PE sheets of the coupled  $^1\pi\pi^*$ - $^1\pi\sigma^*$  states (red colored curve in Fig. 4), display a barrier in the vicinity of the conical intersections. We have evaluated this barrier by breaking the  $C_s$  symmetry of system, to permit vibronic coupling between  $^1\pi\pi^*$  and  $^1\pi\sigma^*$  states. The barrier has been determined to be 0.57, and 0.30 eV, respectively for HQ and CTC systems.

The barrier associated with both systems are smaller than the corresponding barrier, determined for phenol, by Sobolewski and Domcke<sup>11</sup> (~0.90 eV). The smaller barrier before  $S_1/S_0$  conical intersection may provide the faster relaxation to the ground state (i.e the shorter  $S_1$ -lifetime). Sur<sup>70</sup> and later Livingstone<sup>71</sup> estimated the fluorescence lifetime of isolated phenol, to be in the order of 1 nano second. While the lifetime of the 0–0 transition in Hydroquinone and Catechol have been reported to be 480 ps and 7 ps respectively (very shorter than that of phenol)<sup>71</sup>. The shorter lifetime of Catechol has been justified by C. Jouvét<sup>45</sup> and coworkers, by the small  $^1\pi\pi^*/^1\pi\sigma^*$  energy gap. Also, according to Livingstone and coworkers<sup>71</sup>, it may be attributed to differences in the H atom tunneling rate through the barrier formed by a conical intersection between the  $S_1$  ( $^1\pi\pi^*$ ) state and the close lying  $S_2$  ( $^1\pi\sigma^*$ ) state, which is dissociative along the O–H stretching coordinate.

Moreover, it is shown in Figure 4 that the repulsive  $^1\pi\sigma^*$  potential energy profiles intersect the PE profiles of the ground states at OH distances of about 1.9 and 1.8 Å, respectively, for HQ and CTC cases, resulting in the second conical intersection, which is expected to lead the excited system to an ultrafast internal conversion to the ground state.

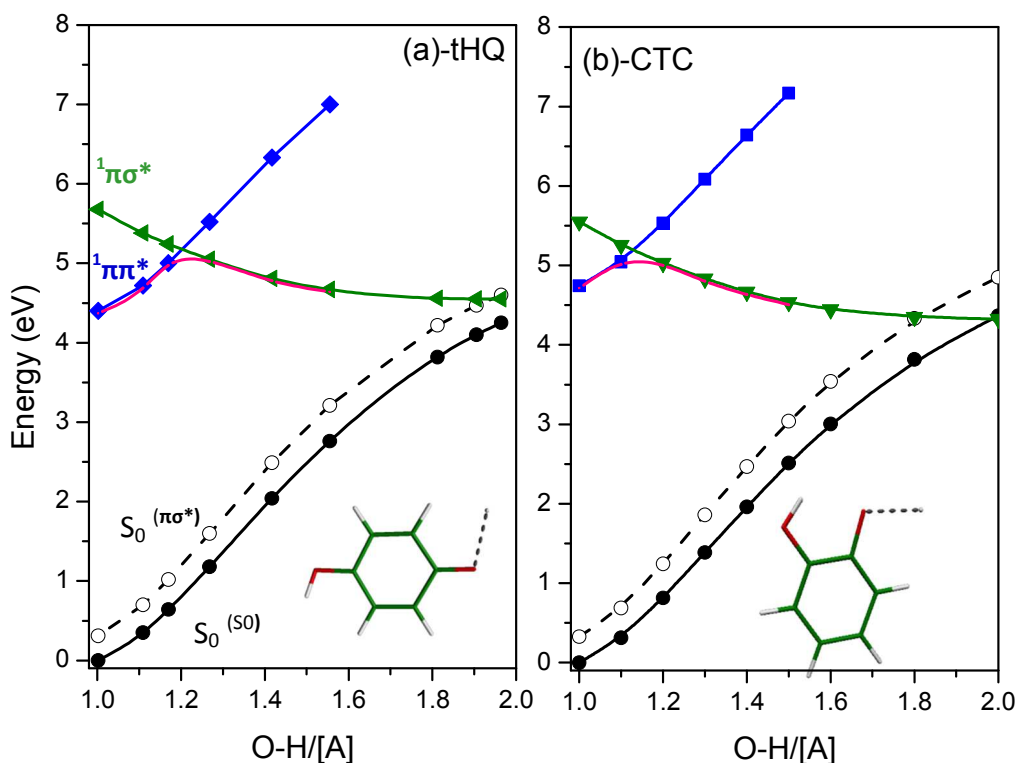


Figure 4: CC2 PE profiles of (a) *trans*-Hydroquinone (*t*-HQ) and (b) Catechol (CTC) in the electronic ground state (circles), the lowest  $^1\pi\pi^*$  state (squares) and the lowest  $^1\pi\sigma^*$  excited state (triangles), as a function of the OH stretching coordinate. The energy profiles of reaction pathways determined in the same electronic state ( $S_0^{(S_0)}$ ) have been represented by full lines, while the energy profiles of reaction paths calculated at the complementary electronic states ( $S_0^{(S_1)}$ ,  $S_1^{(S_0)}$ ) have been shown by dashed lines. In addition, the red colored curves in both panels represent the PE profile of  $S_1$  state without  $C_s$  symmetry constraint.

### 3-C-II) Hydroquinone and Catechol clusters with two ammonia molecules:

The CC2 geometry optimization of HQ-,CTC-(NH<sub>3</sub>)<sub>2</sub>, at the  $S_2$  ( $^1\pi\sigma^*$ ) state leads to the single hydrogen transfer between OH groups of HQ/CTC and ammonia molecules. In contrast to HQ-(NH<sub>3</sub>)<sub>2</sub>, the  $\sigma^*$  orbital of CTC-(NH<sub>3</sub>)<sub>2</sub> is mostly located on one of ammonia molecules, (see Figure 5). Thus, the single hydrogen transfer process at the  $^1\pi\sigma^*$  state in CTC-(NH<sub>3</sub>)<sub>2</sub> is justified, since of the  $\sigma^*$  electron distribution.

The CC2 PE profiles calculated along the minimum-energy path for hydrogen transfer between tHQ, CTC and ammonia are presented in Figure 6. The reaction coordinates are defined as the difference between the O-H and N-H bond distances and describe the position of the hydrogen relative to the oxygen atom and ammonia, respectively. As shown in Figure 6, the main effect of complexation of HQ/CTC with two ammonia molecules is the removal of the conical intersection of the  $^1\pi\sigma^*$  state with the  $S_0$  state, which is in good agreement with the result of Sobolewski and Domcke<sup>11</sup> on the phenol-ammonia clusters. In comparison with Figure 4, the  $^1\pi\sigma^*$  energy is moved slightly downward, nevertheless, the  $S_0$  energy increases significantly less than in bare molecules for large OH distances. As a result, the  $^1\pi\sigma^*$  state shows a minimum at about  $R_{HT} \sim 0.8$  Å and the intersection with the ground state is removed. At the minimum, hydrogen of the phenolic OH group is transferred to the ammonia molecule. The ultrafast internal-conversion channel which exists in the bare HQ/CTC systems is thus eliminated in the cluster systems with two ammonia molecules. However, when the  $C_s$  symmetry is not imposed on determination of the  $S_1$  potential energy curves, the  $S_1$  PE profiles of both clustered systems show a barrier along the HT reaction coordinate. This barrier has been evaluated to be 0.86 eV and 0.31 eV in the tHQ-(NH<sub>3</sub>)<sub>2</sub> and CTC-(NH<sub>3</sub>)<sub>2</sub>, respectively, which indicate that HT process in the later complex is faster.

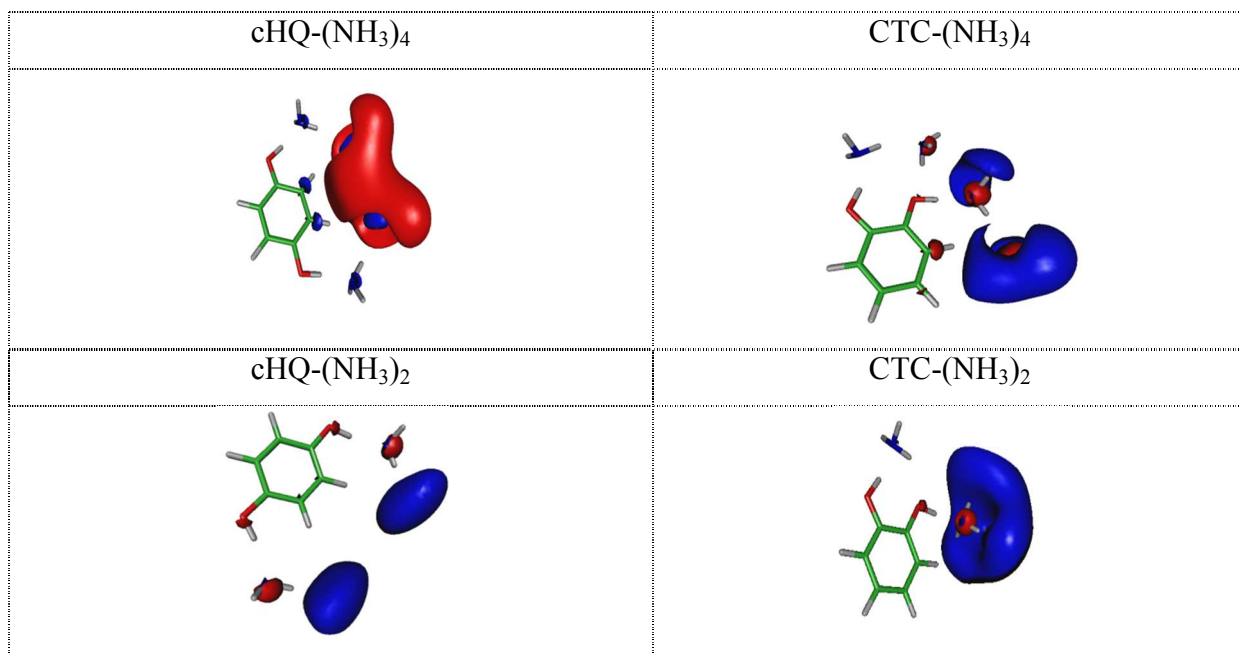


Figure 5: Visualized  $\sigma^*$  orbital of cHQ-(NH<sub>3</sub>)<sub>2,4</sub> and CTC-(NH<sub>3</sub>)<sub>2,4</sub> systems.

### 3-C-III) Hydroquinone and catechol clusters with four ammonia molecules:

The CC2 geometry optimization of cHQ-(NH<sub>3</sub>)<sub>4</sub> and CTC-(NH<sub>3</sub>)<sub>4</sub>, at the S<sub>2</sub> (<sup>1</sup> $\pi\sigma^*$ ) state leads to the double hydrogen transfer (DHT) from OH groups of HQ/CTC to the adjacent ammonia molecules (ESI file). Figure 5, represents the  $\sigma^*$  orbitals of these systems, mostly located on the two ammonia, having the largest distance to HQ and CTC. Thus, double hydrogen transfer (DHT) has been expected to occur following the charge transfer from  $\pi$  orbital (located on the benzene ring) to the  $\sigma^*$  orbital on solvent. Consequently, the HT process in cluster systems of cHQ-(NH<sub>3</sub>)<sub>4</sub>/CTC-(NH<sub>3</sub>)<sub>4</sub> is essentially different from their corresponding smaller systems (n<4). The exact estimation of double hydrogen transfer process requires a 2-dimensional (2D) potential energy surface exploration<sup>72</sup>. However, due to the importance of this phenomenon, we have determined a qualitatively feature of DHT on clusters of HQ and CTC with ammonia.

In Figure 7, the qualitative CC2 PE profiles calculated along the energy path for concerted shifting of phenolic hydrogens to adjacent ammonia molecules have been presented. The reaction coordinates are defined as the difference between the O-H and N-H bond lengths, from

both sides of clusters, and describe the position of the hydrogen atoms relative to the oxygen atoms.

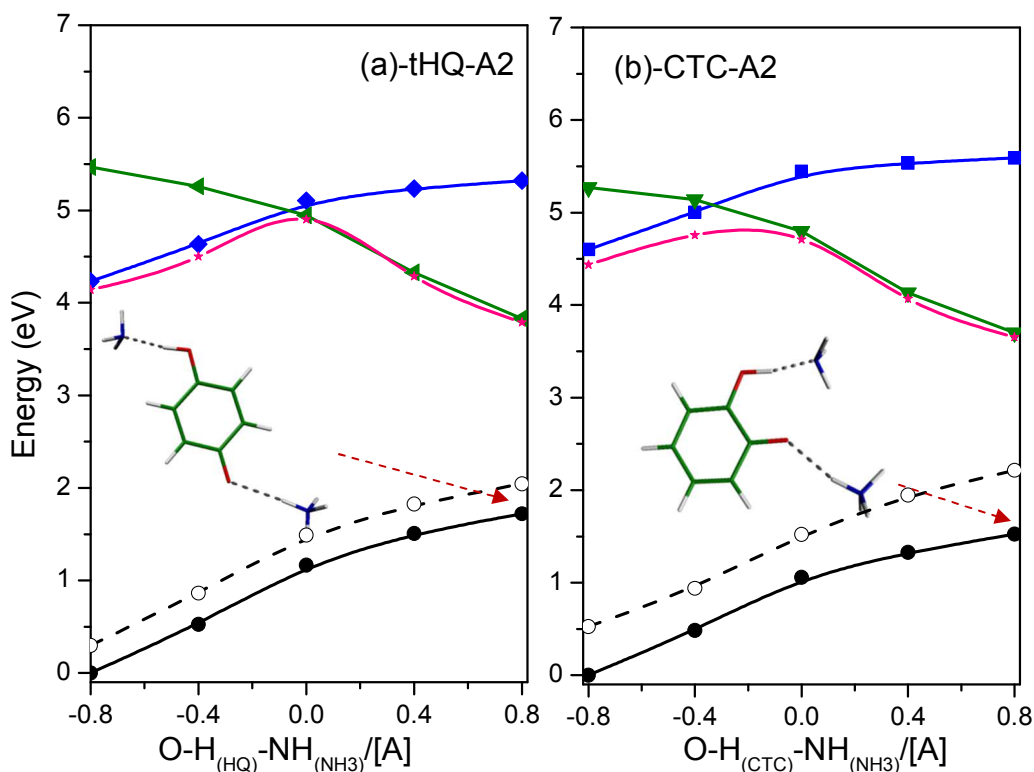


Figure 6: CC2 PE profiles of di-ammoniated clusters of (a) trans-Hydroquinone (t-HQ) and (b) Catechol (CTC) in the electronic ground state (circles), the lowest  ${}^1\pi\pi^*$  excited state (squares), the lowest  ${}^1\pi\sigma^*$  state (triangles), as a function of the hydrogen-transfer reaction coordinate. The pink-color curves in both panels represent the PE profile of  $S_1$  state without  $C_s$  symmetry constraint.

It is seen that the PE profiles of the ground state and the lowest  ${}^1\pi\pi^*$  excited state rise with increasing the reaction coordinate, while the  ${}^1\pi\sigma^*$  profile has a flat pattern at the beginning of reaction path and after that, it decreases. These trends lead to the conical intersections of  ${}^1\pi\pi^*$ - ${}^1\pi\sigma^*$  at the beginning of the reaction coordinate, for both clustered systems of  $cHQ-(NH_3)_4$  and  $CTC-(NH_3)_4$ . As shown in Figure 7, the complexation of HQ/CTC with four ammonia molecules significantly decreases the  ${}^1\pi\pi^*$ - ${}^1\pi\sigma^*$  energy and consequently the potential energy barrier of the  $S_1$  state. In the DHT reaction coordinates, in contrast to single HT in mono- and di-ammoniated systems, there is a conical intersection between the  ${}^1\pi\sigma^*$  and  $S_0$  states, indicating to different



photophysical behavior of excited tetra-ammoniated systems. It is shown in Figure 7 that repulsive  ${}^1\pi\sigma^*$  PE profiles intersect the PE profiles of the ground state at OH distances of about 1.8 and 1.9 Å respectively for HQ-(NH<sub>3</sub>)<sub>4</sub> and CTC-(NH<sub>3</sub>)<sub>4</sub> cases, resulting in the second conical intersection, which is expected to lead the excited system to the ground state via internal conversion. This internal conversion can be responsible for ultrafast deactivation of photoexcited HQ-(NH<sub>3</sub>)<sub>4</sub> and CTC-(NH<sub>3</sub>)<sub>4</sub> systems.

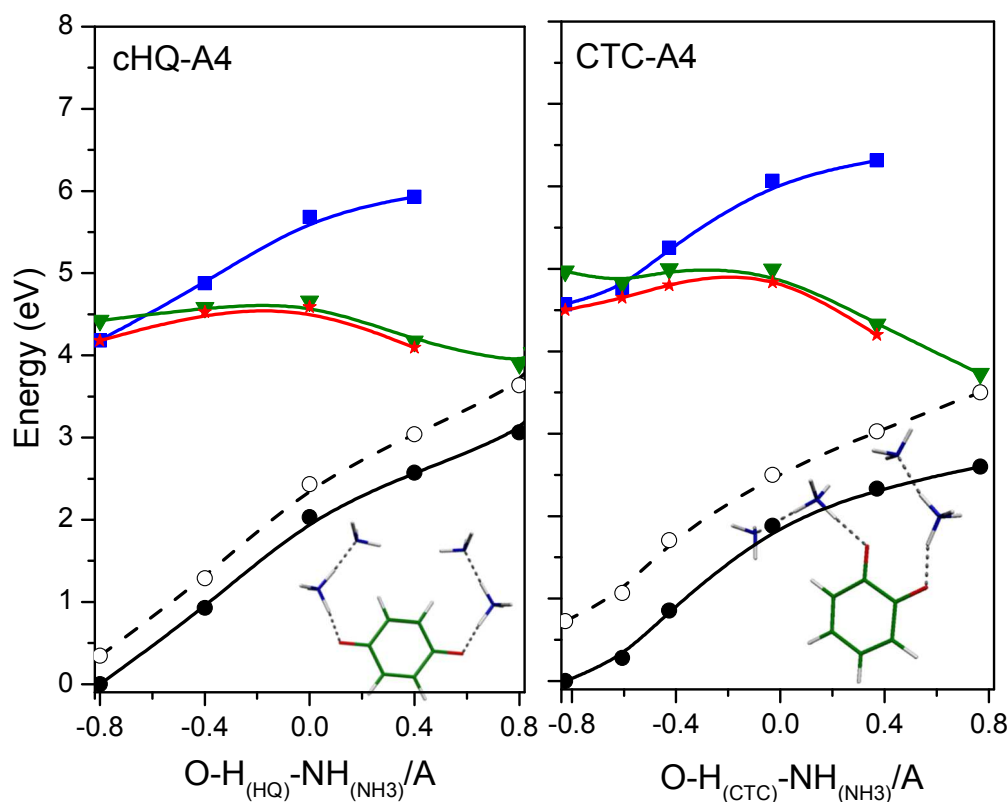


Figure 7: Potential energy profiles of tetra-ammoniated clusters of (a) *cis*-Hydroquinone (tHQ) and (b) Catechol (CTC) molecules in the electronic ground state (circles), the lowest  ${}^1\pi\pi^*$  excited state (squares), and the lowest  ${}^1\pi\sigma^*$  state (triangles), as a function of the hydrogen-transfer reaction coordinate. The red-color curves in both panels represent the PE profile of  $S_1$  state without  $C_s$  symmetry constraint.

#### 4- Conclusion

*Ab initio* electronic-structure and reaction-path calculations have been performed to characterize the hydrogen detachment process in bare Hydroquinone/Catechol and intracluster hydrogen transfer processes in their clusters with ammonia. It has been found that the lowest  $^1\pi\sigma^*$  state plays a prominent role in the photochemistry of these systems. In the bare molecules, the  $^1\pi\sigma^*$  state predissociates the bound  $S_1$  ( $^1\pi\pi^*$ ) state, and forms a conical intersection with the ground state. For the cases of HQ/CTC, clustered with four ammonia molecules, double hydrogen transfer has been predicted along the O-H stretching coordinates in the  $^1\pi\sigma^*$  state. In this reaction coordinate, the  $^1\pi\sigma^*$  state predissociates the bound  $S_1$  ( $^1\pi\pi^*$ ) state, and connects the  $S_1$  state to a conical intersection with the  $S_0$  state. This conical intersection provides the main pathway for ultrafast deactivation of excited systems to the ground state. Nevertheless, clustering of Hydroquinone/Catechol with two ammonia molecules, eliminates the  $^1\pi\sigma^*$ - $S_0$  conical intersection in the reaction coordinate of single hydrogen transfer.

#### Acknowledgment

The research council of *Isfahan University* is acknowledged for financial support. We acknowledge the use of the computing facility cluster GMPCS of the LUMAT federation (*FR LUMAT 2764*).

**References:**

1. A. L. Sobolewski, W. Domcke, C. Dedonder-Lardeux and C. Jouvet, *Phys. Chem. Chem. Phys.*, 2002, **4**, 1093-1100.
2. J. Steadman and J. A. Syage, *J. Chem. Phys.*, 1990, **92**, 4630-4632.
3. J. A. Syage, *Chem. Phys. Lett.*, 1993, **202**, 227-232.
4. J. A. Syage and J. Steadman, *J. Phys. Chem.*, 1992, **96**, 9606-9608.
5. A. L. Sobolewski and W. G. Domcke, *J. Phys. Chem. A*, 2007, **111**, 11725-11735.
6. A. R. Morales, K. J. Schafer-Hales, C. O. Yanez, M. V. Bondar, O. V. Przhonska, A. I. Marcus and K. D. Belfield, *ChemPhysChem*, 2009, **10**, 2073-2081.
7. T. I. Kim, H. J. Kang, G. Han, S. J. Chung and Y. Kim, *Chem. Comm.*, 2009, 5895-5897.
8. F. S. Rodembusch, F. P. Leusin, L. F. da Costa Medina, A. Brandelli and V. Stefani, *Photoch. Photobio. Sci.*, 2005, **4**, 254-259.
9. M. Zimmer, *Chem. Rev.*, 2002, **102**, 759-781.
10. Z. Lan, W. Domcke, V. Vallet, A. L. Sobolewski and S. Mahapatra, *J. Chem. Phys.*, 2005, **122**, 224315.
11. A. L. Sobolewski and W. Domcke, *J. Phys. Chem. A*, 2001, **105**, 9275-9283.
12. M. N. R. Ashfold, B. Cronin, A. L. Devine, R. N. Dixon and M. G. D. Nix, *Science*, 2006, **312**, 1637-1640.
13. C.-M. Tseng, Y. T. Lee, M.-F. Lin, C.-K. Ni, S.-Y. Liu, Y.-P. Lee, Z. F. Xu and M. C. Lin, *J. Phys. Chem. A*, 2007, **111**, 9463-9470.
14. D. Creed, *Photochem. Photobiol.*, 1984, **39**, 537-562.
15. M. G. D. Nix, A. L. Devine, B. Cronin, R. N. Dixon and M. N. R. Ashfold, *J. Chem. Phys.*, 2006, **125**, 133318.
16. A. L. Devine, M. G. D. Nix, B. Cronin and M. N. R. Ashfold, *Phys. Chem. Chem. Phys.*, 2007, **9**, 3749-3762.
17. M. N. R. Ashfold, A. L. Devine, R. N. Dixon, G. A. King, M. G. D. Nix and T. A. A. Oliver, *P. Nat. Acad. Sci. USA*, 2008, **105**, 12701-12706.
18. T. Burgi, T. Droz and S. Leutwyler, *Chem. Phys. Lett.*, 1995, **246**, 291-299.
19. O. David, C. Dedonder-Lardeux and C. Jouvet, *Int. Rev. Phys. Chem.*, 2002, **21**, 499-523.
20. G. Grégoire, C. Dedonder-Lardeux, C. Jouvet, S. Martrenchard and D. Solgadi, *J. Phys. Chem. A*, 2001, **105**, 5971-5976.
21. D. Henseler, C. Tanner, H. M. Frey and S. Leutwyler, *J. Chem. Phys.*, 2001, **115**, 4055-4069.
22. C. Jouvet, C. Lardeuxdedonder, M. Richardviard, D. Solgadi and A. Tramer, *J. Phys. Chem.*, 1990, **94**, 5041-5048.
23. G. Pino, G. Gregoire, C. Dedonder-Lardeux, C. Jouvet, S. Martrenchard and D. Solgadi, *Phys. Chem. Chem. Phys.*, 2000, **2**, 893-900.
24. O. Cheshnovsky and S. Leutwyler, *Chem. Phys. Lett.*, 1985, **121**, 1-8.
25. S. K. Kim, J. K. Wang and A. H. Zewail, *Chem. Phys. Lett.*, 1994, **228**, 369-378.
26. G. Gregoire, C. Dedonder-Lardeux, C. Jouvet, S. Martrenchard, A. Peremans and D. Solgadi, *J. Phys. Chem. A*, 2000, **104**, 9087-9090.
27. S.-i. Ishiuchi, K. Daigoku, M. Saeki, M. Sakai, K. Hashimoto and M. Fujii, *J. Chem. Phys.*, 2002, **117**, 7077-7082.
28. G. A. Pino, A. N. Oldani, E. Marceca, M. Fujii, S.-i. Ishiuchi, M. Miyazaki, M. Broquier, C. Dedonder and C. Jouvet, *J. Chem. Phys.*, 2010, **133**, 124313-124325.
29. C. Dedonder-Lardeux, D. Grosswasser, C. Jouvet and S. Martrenchard, *PhysChemComm*, 2001, **4**, 21-23.

30. S.-i. Ishiuchi, M. Sakai, K. Daigoku, K. Hashimoto and M. Fujii, *J. Chem. Phys.*, 2007, **127**, 234304-232343?
31. A. L. Sobolewski, *J. Photochem. Photobiol. A*, 1995, **89**, 89-97.
32. O. David, C. Dedonder-Lardeux, C. Jouvét, H. Kang, S. Martrenchard, T. Ebata and A. L. Sobolewski, *J. Chem. Phys.*, 2004, **120**, 10101-10110.
33. B. Halliwell, R. Aeschbach, J. Löliger and O. I. Aruoma, *Food Chem. Toxicol.*, 1995, **33**, 601-617.
34. H. H. Hussain, G. Babic, T. Durst, J. S. Wright, M. Flueraru, A. Chichirau and L. L. Chepelev, *J. Org. Chem.*, 2003, **68**, 7023-7032.
35. C. A. Beck, *J. Chem. Phys.*, 1950, **18**, 1135-1142.
36. T. M. Dunn, R. Tembreull and D. M. Lubman, *Chem. Phys. Lett.*, 1985, **121**, 453-457.
37. T. Bürgi and S. Leutwyler, *J. Chem. Phys.*, 1994, **101**, 8418-8429.
38. M. Gerhards, S. Schumm, C. Unterberg and K. Kleinermanns, *Chem. Phys. Lett.*, 1998, **294**, 65-70.
39. M. Gerhards, C. Unterberg and S. Schumm, *J. Chem. Phys.*, 1999, **111**, 7966-7975.
40. R. Tembreull, T. M. Dunn and D. M. Lubman, *Spectrochim. Acta A*, 1986, **42**, 899-906.
41. W. Caminati and S. Di Bernardo, *J. Mol. Struct.*, 1990, **240**, 263-274.
42. M. Onda, K. Hasunuma, T. Hashimoto and I. Yamaguchi, *J. Mol. Struct.*, 1987, **159**, 243-248.
43. M. Gerhards, W. Perl and K. Kleinermanns, *Chem. Phys. Lett.*, 1995, **240**, 506-512.
44. G. A. King, T. A. A. Oliver, R. N. Dixon and M. N. R. Ashfold, *Phys. Chem. Chem. Phys.*, 2012, **14**, 3338-3345.
45. M. Weiler, M. Miyazaki, G. Féraud, S.-i. Ishiuchi, C. Dedonder, C. Jouvét and M. Fujii, *J. Phys. Chem. Lett.*, 2013, **4**, 3819-3823.
46. R. Ahlrichs, M. Bär, M. Häser, H. Horn and C. Kölmel, *Chem. Phys. Lett.*, 1989, **162**, 165-169.
47. TURBOMOLE, V6.3 2011, a development of University of Karlsruhe and Forschungszentrum Karlsruhe GmbH, 1989-2007, TURBOMOLE GmbH, since 2007; available from <http://www.turbomole.com>.
48. F. Haase and R. Ahlrichs, *J. Comput. Chem.*, 1993, **14**, 907-912.
49. C. Hattig and K. Hald, *Phys. Chem. Chem. Phys.*, 2002, **4**, 2111-2118.
50. R. A. Kendall, T. H. Dunning and R. J. Harrison, *J. Chem. Phys.*, 1992, **96**, 6796-6806.
51. I. Alata, R. Omidyan, C. Dedonder-Lardeux, M. Broquier and C. Jouvét, *Phys. Chem. Chem. Phys.*, 2009, **11**, 11479-11486.
52. I. Alata, R. Omidyan, M. Broquier, C. Dedonder, O. Dopfer and C. Jouvét, *Phys. Chem. Chem. Phys.*, 2010, **12**, 14456-14458.
53. G. Gregoire, C. Jouvét, C. Dedonder and A. L. Sobolewski, *J. Am. Chem. Soc.*, 2007, **129**, 6223-6231.
54. M. Schreiber, M. R. Silva-Junior, S. P. A. Sauer and W. Thiel, *J. Chem. Phys.*, 2008, **128**, -.
55. J. Jankowska, M. F. Rode, J. Sadlej and A. L. Sobolewski, *ChemPhysChem*, 2012, **13**, 4287-4294.
56. J. Jankowska, M. F. Rode, J. Sadlej and A. L. Sobolewski, *ChemPhysChem*, 2014, **15**, 1643-1652.
57. A. L. Sobolewski and W. Domcke, *Phys. Chem. Chem. Phys.*, 2006, **8**, 3410-3417.
58. A. L. Sobolewski and W. Domcke, *ChemPhysChem*, 2007, **8**, 756-762.
59. W. Caminati, S. Melandri and L. B. Favero, *J. Chem. Phys.*, 1994, **100**, 8569-8572.
60. K. Kim and K. D. Jordan, *Chem. Phys. Lett.*, 1995, **241**, 39-44.
61. C. Puebla and T.-K. Ha, *J. Mol. Struct.*, 1990, **204**, 337-351.
62. Y. Song, J. Xie, H. Shu, G. Zhao, X. Lv and H. Cai, *Bioorgan. Med. Chem.*, 2005, **13**, 5658-5667.
63. T. K. Manojkumar, Kim, D., Kim, K.S. *J. Phys. Chem.*, 2005, **122**, 014305.
64. M. Gerhards, M. Schiwiek, C. Unterberg and K. Kleinermanns, *Chem. Phys. Lett.*, 1998, **297**, 515-522.

65. H. W. Wilson, *Spectrochim. Acta A-M*, 1974, **30**, 2141-2152.
66. H. G. Kjaergaard, D. L. Howard, D. P. Schofield, T. W. Robinson, S.-i. Ishiuchi and M. Fujii, *J. Phys. Chem. A*, 2001, **106**, 258-266.
67. S. J. Humphrey and D. W. Pratt, *J. Chem. Phys.*, 1993, **99**, 5078-5086.
68. P. S. Meenakshi, N. Biswas and S. Wategaonkar, *Phys. Chem. Chem. Phys.*, 2003, **5**, 294-299.
69. K. Sundaram and W. P. Purcell, *Int. J. Quantum Chem.*, 1971, **5**, 101-110.
70. A. Sur and P. M. Johnson, *J. Chem. Phys.*, 1986, **84**, 1206-1209.
71. R. A. Livingstone, J. O. F. Thompson, M. Iljina, R. J. Donaldson, B. J. Sussman, M. J. Paterson and D. Townsend, *J. Chem. Phys.*, 2012, **137**, 184304-184321.
72. K. Ando, S. Hayashi and S. Kato, *Phys. Chem. Chem. Phys.*, 2011, **13**, 11118-11127.